JOURNAL OF APPLIED POLYMER SCIENCE VOL. 14, PP. 285-301 (1970)

Polyacrylic Desalination Membranes. II. Reverse Osmosis Performance

ALLAN S. HOFFMAN, MICHAEL MODELL, and PETER PAN,
Department of Chemical Engineering, Massachusetts Institute of Technology, Cambridge, Massachusetts 02139

Synopsis

A new class of polyacrylic membranes has been tested under reverse osmosis conditions on dilute (1%–4%) salt solutions. Fluxes up to 0.2 gal-mil/ft²-day at greater than 98% rejection have been achieved. The effect of membrane composition on product flux and salt rejection is discussed. Increased fluxes at even higher rejection should be possible by proper selection of the type and concentration of hydrophilic, hydrophobic, and crosslinking monomers. It is concluded that improved membranes should have as high as possible a concentration of hydrophilic groups, distributed randomly through a lightly crosslinked, rubbery polymer matrix.

INTRODUCTION

In the first part of this investigation,[1] the synthesis and characterization of a new class of polyacrylic desalination membranes have been described. These membranes are composed of hydrophilic, hydrophobic, and crosslinking monomers and are synthesized by polymerizing the monomer mixtures in film form. The details of synthesis and water and salt sorption data are presented in part I.[1] In this part, the reverse osmosis performance of these membranes is presented and the effect of membrane composition on the transport mechanisms for salt and water is discussed.

MECHANISM OF DESALINATION

In uncharged membranes which are free of imperfections and pores, the solution–diffusion model has been found to describe adequately salt and water transport.[2–4] In this model, water and salt dissolve in the membrane at the upstream solution–membrane interface and diffuse independently under their respective chemical potential gradients to the downstream solution–membrane interface, where they desorb into the downstream solution. Assuming that salt and water are in equilibrium across each solution–membrane interface, it can be shown[5] that at steady state the water and salt fluxes are given by eqs. (1) and (2), respectively, as follows:

$$J_w = \frac{D_w C_w \bar{V}_w}{RT} \frac{\Delta P - \Delta \pi}{\Delta X} \tag{1}$$

$$J_s = D_s K \frac{\Delta C'_s}{\Delta X} \tag{2}$$

The per cent salt rejection may then be written as

$$\%\text{S.R.} = 100\left[\frac{\Delta C'_s}{C'_{s,0}}\right]$$

$$= 100\left[1 - \frac{J_s}{C'_{s,0}J_w}\right] \quad (\text{if } J_s \ll J_w)$$

$$= 100\left[1 - \left(\frac{D_s K}{D_w C_w}\right)\left(\frac{RT}{\bar{V}_w}\right)\left(\frac{\Delta C'_s}{C'_{s,0}}\frac{1}{\Delta P - \Delta\pi}\right)\right]$$

or

$$\%\text{S.R.} = \frac{100}{\left[1 + \left(\frac{D_s K}{D_w C_w}\right)\left(\frac{RT}{\bar{V}_w}\right)\left(\frac{1}{\Delta P - \Delta\pi}\right)\right]} \tag{3}$$

It can be seen in eq. (3) that for any one set of operating conditions (fixed $C'_{s,0}$ and ΔP) the salt rejection is determined by the ratio of salt-to-water permeabilities in the membrane, $(D_s K)/(D_w C_w)$. This ratio may be split into the product of two terms, $(D_s/D_w) \times (K/C_w)$ or $(D_s/D_w) \times (K^*)$. The first term, the diffusivity ratio, may be interpreted as the "kinetic" factor and the second term, K^*, as the "equilibrium" factor governing permselectivity.

TABLE I
Composition of Membrane Synthesis Solutions[1,a]

Membrane no.	EA, mole-%	TPT, mole-%	Heat treatment
E-1	10.2	0	IR lamp
E-2	18.7	0	IR lamp
E-3	25.6	0	IR lamp
E-4	31.4	0	IR lamp
E-6	40.7	0	IR lamp
ET-01	0	4.0	oven
ET-11	9.9	3.6	oven
ET-21(TE-12)	18.0	3.3	oven
ET-21X	18.0	3.3	none
ET-31	24.8	3.0	oven
TE-02	18.7	0	oven
TE-12(ET-21)	18.0	3.3	oven
TE-22	17.6	6.5	oven
TE-32	16.9	9.4	oven

[a] All solutions contained H_2O, AAc, and NMA in mole ratios of 19:12:5. See *Nomenclature* for identification of all symbols.

PROCEDURE

Membrane Compositions

Table I summarizes the compositions of the membranes studied here.

Dye Test for Imperfections

The membranes selected for test under reverse osmosis were first screened to be sure that they were free of holes or other such imperfections. They were placed on the upstream side of a two-chamber filtration cell on top of three pieces of filter paper and over a sintered metal disc. Then a few cc's of aqueous solution of acid red fuchsin dye were added to the upstream chamber and the downstream chamber was placed under vacuum. Any holes or defects in the membrane were seen as red spots on the filter papers and the membrane was not used if such spots appeared. In the absence of such spots, the membrane was washed and then soaked in fresh distilled water for two days before testing under reverse osmosis conditions.

Reverse Osmosis Tests

Membranes approximately 2.5 in. in diameter were placed smooth side up in the desalination cell shown in Figure 1. The "smooth side" refers to the side of the membrane against the glass surface during polymerization (see part I[1]). They were then tested as reverse osmosis membranes under pressures between 800–1500 psig with salt solutions of 1% or 4% NaCl. These tests were all at 25°C and pH 4.0; the latter condition assured that the AAc groups were not ionized to any great extent. To minimize membrane fouling associated with solubilized corrosion products, the solutions were fed to the pump containing small amounts of dissolved ethylenediaminetetracetic acid (EDTA) (200 ppm in 1% solution and 250 ppm in 4% solution). Usually, it was necessary to run for many days (and sometimes for several weeks) before the product flow rate and salt concentration attained steady state. A typical example of this behavior is illustrated in Figure 2. Note that both water flux and salt rejection increase with time during the transient. Thus, the transient cannot be attributed to formation of a dynamic membrane (e.g., resulting from the addition of EDTA), nor is it likely to be the result of compaction. When the cell was opened after such a run, there was generally very little "scum" to be seen on the upstream membrane surface.

The product stream was collected in a graduate closed over with aluminum foil and sample volumes were removed for "average" analyses of salt concentration every few days. Product flux J_w is converted from (cc/hr) to (gal-mil/ft^2-day) by multiplying by 0.258 $\times$ (film thickness). In some cases, J_w is not normalized with respect to thickness and is reported directly as g/cm^2-sec.

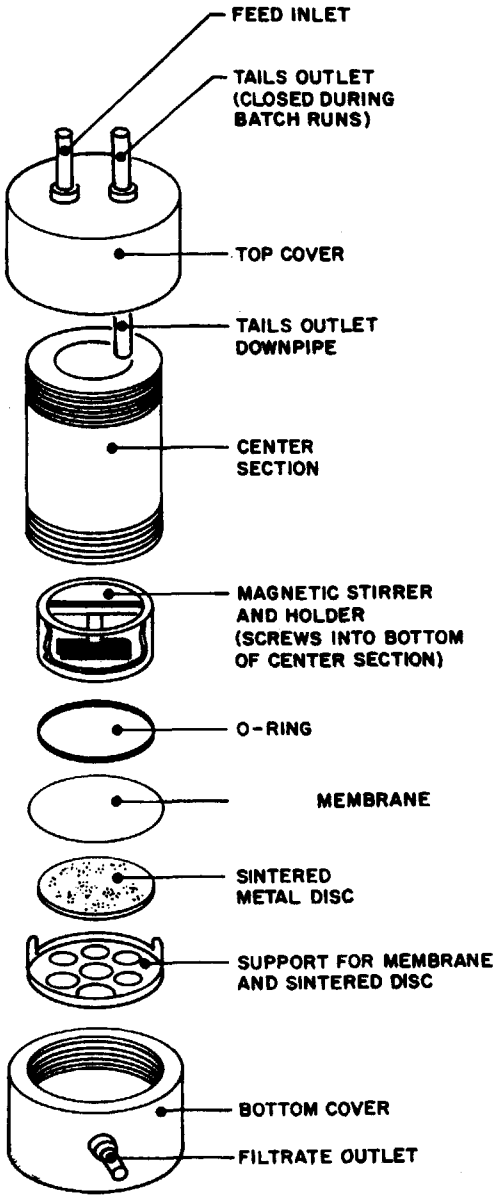

Fig. 1. Desalination cell.

The salt concentrations in these samples were obtained by measuring conductivity and converting to concentration by use of a calibration curve. Per cent salt rejection, %S.R., was calculated as 100 ($\Delta C'_s/C'_{s,0}$).

Calculated Values

Apparent water and salt permeabilities, D_wC_w and D_sK, respectively, were calculated from the measured quantities, using the solution–diffusion

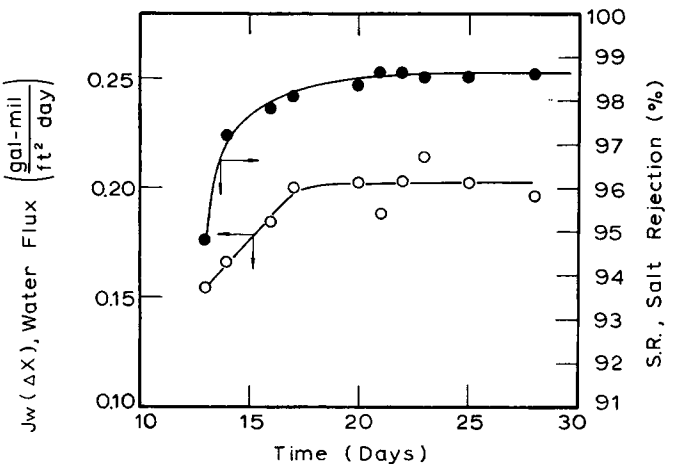

Fig. 2. Water flux (○) and salt rejection (●) as a function of time on stream. Membrane ET-31 with 1.0 wt-% NaCl at 1500 psig.

transport equations presented above. Values for C_w were calculated from measured values of C_w^* by assuming that the specific volume of the wet membrane is the weighted sum of the specific volumes of water and the dry membrane. The latter was assumed to vary linearly with TPT content, varying from 0.83 for no TPT to 0.74 for membranes containing 9.4 mole-% TPT. The molar salt distribution coefficient, K, was calculated from the measured values of K^* and the calculated values of C_w by the approximation $K \cong C_w K^*$. Diffusivities of water and salt were then calculated from the apparent permeabilities, assuming that the values of C_w and K, which were estimated from ambient pressure measurements of C_w^* and K^*, would not be significantly affected by the higher pressures of reverse osmosis tests.

RESULTS

Membrane Compaction and "Pore Flow" Under Reverse Osmosis

A series of reverse osmosis tests was first run at both varying $\Delta\pi$ and ΔP to determine the significance of compaction and pore flow in the membrane. A summary of these data is presented in Table II. The normalized product of water flux divided by $\Delta P(C'_w)_0$ is plotted against $(\Delta P - \Delta\pi)/(\Delta P(C'_w)_0)$ for the ET-21 and ET-21X membranes in Figure 3. The approximately linear relationship indicates the probable absence of significant pressure-induced compaction of the membranes. Since the extrapolated intercept in Figure 3 appears to be close to the origin, the contribution of "pore flow" to the overall water flux is not significant. The approximate linearity of the data and the intersection at the origin indicate that $D_w C_w$ is independent of salt concentration and hydrostatic pressure. Since this result was found for several membranes, $D_w C_w$ values were determined in later runs from

TABLE II
Effect of Varying Hydrostatic ΔP or Solution $\Delta\pi$ on Reverse Osmosis Performance[a]

Membrane no.	ΔX, mils	$C'_{s,0}$ wt-%	$\Delta\pi$, psig	ΔP, psig	$J_w\Delta X$, (gal-mil)/-(ft²-day)	S.R., %	D_wC_w, gram/cm-sec	D_sK, cm²/sec
ET-21 (a1)	7.0	1.0	106.5	800	0.13	96.6	4.6×10^{-7}	5.4×10^{-10}
ET-21 (a2)	7.0	1.0	107.0	1200	0.20	97.1	4.3×10^{-7}	7.0×10^{-10}
ET-21 (a3)	7.0	1.0	107.8	1500	0.26	97.8	4.4×10^{-7}	6.8×10^{-10}
ET-21 (a4)	7.0	4.0	422.5	1500	0.20	94.0	4.3×10^{-7}	[b]1.4×10^{-9}
ET-21 (b)	8.4	4.0	425.5	1500	0.19	94.5	4.2×10^{-7}	[b]1.3×10^{-9}
TE-02 (a)	5.7	1.0	91.5	800	0.65	84.0	2.2×10^{-6}	1.7×10^{-8}
TE-02 (b1)	7.1	1.0	99.7	1200	1.04	90.2	2.3×10^{-6}	1.3×10^{-8}
TE-02 (b2)	7.1	1.0	100.8	1500	1.19	91.5	2.0×10^{-6}	1.3×10^{-8}
ET-21X (a)	6.6	1.0	104.2	800	0.15	94.6	5.2×10^{-7}	1.0×10^{-9}
ET-21X (b)	6.6	1.0	105.8	1200	0.20	96.1	4.4×10^{-7}	9.8×10^{-10}
ET-21X (c)	6.6	1.0	107.3	1500	0.26	97.6	4.5×10^{-7}	8.0×10^{-10}
ET-21X (d)	6.6	4.0	417.0	1500	0.18	92.7	4.1×10^{-7}	[b]1.7×10^{-9}

[a] See *Nomenclature* for explanation of symbols.
[b] Determined from one-point ratio (see text).

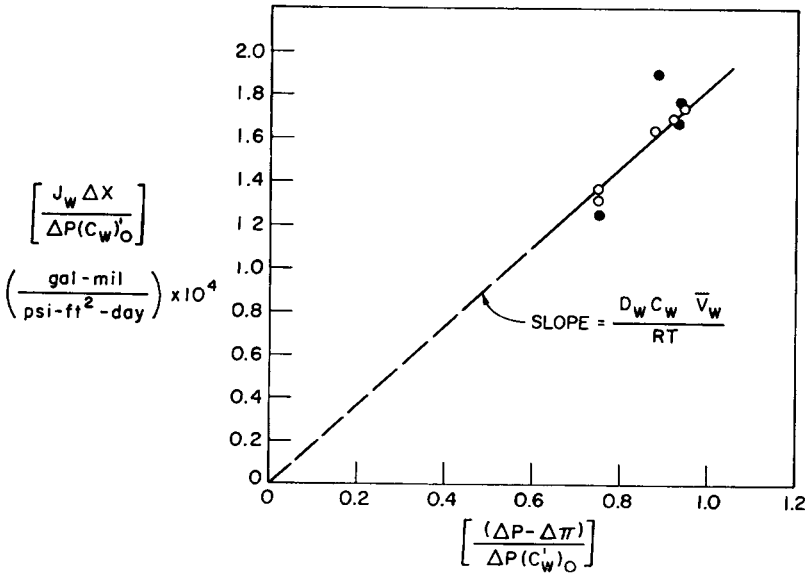

Fig. 3. Effect of ΔP and $\Delta \pi$ on normalized product water flux: (O) ET-21; (●) ET-21X.

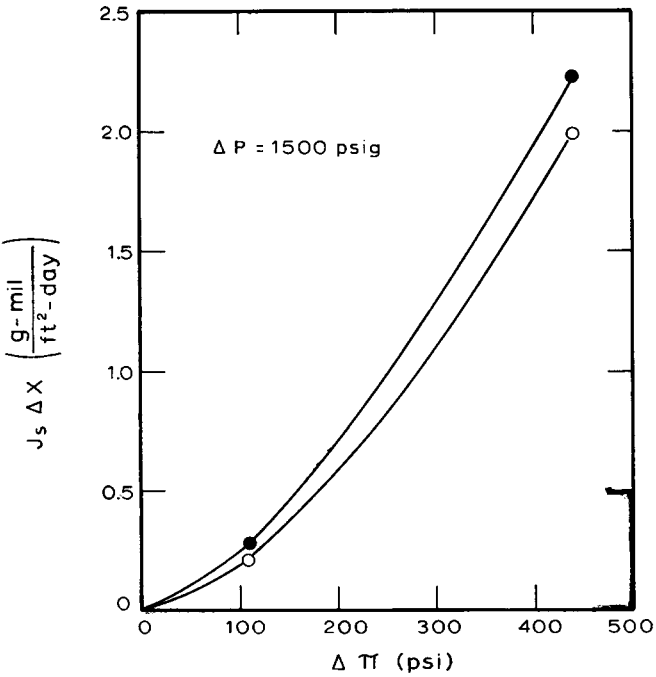

Fig. 4. Effect of $\Delta \pi$ on normalized salt flux: (O) ET-21 (a3 and a4); (●) ET-21X (c and d).

one-point ratios of $[J_w(\Delta X)]/(\Delta P - \Delta\pi)$ obtained at one ΔP and one salt concentration.

It should also be noted in Table II that in several cases membranes were prepared in separate polymerizations from freshly prepared monomer mixtures, and the reverse osmosis data for these membranes appear to be internally consistent and reproducible. This demonstrates the reproducibility of membrane preparation as well as of the reverse-osmosis testing procedures.

It may also be noted that the values for salt flux, J_s, in the runs at 1.0% salt concentration are essentially independent of ΔP between 800 and 1500 psig. This would be expected if there were no compaction of the membranes under pressure. However, when salt concentration was increased in two cases from 1.0% to 4.0%, a plot of normalized salt flux $J_s(\Delta X)$ versus $\Delta\pi$ is not linear (Fig. 4). This indicates that salt diffusivity, D_s, is increasing as the external solution concentration increases. Since the water and salt contents inside these membranes do not appear to change significantly between 1.0% and 4.0% salt in the external solution,[1] it is not clear why D_s inside the membrane should be increasing over this range. For this reason, the calculated values of D_sK or D_s obtained by one-point ratios of $[J_s(\Delta X)]/(\Delta C'_s)$ may be less than the true value; these runs are so indicated in Table II. (It is possible that in the long-time reverse-osmosis tests there is a slight increase in upstream brine pH with time, due to corrosion; this could lead to a slightly greater ionization of the $-CO_2H$ groups at 4% upstream salt concentration than at 1%, leading to somewhat greater swelling and higher D_s values.)

Reverse Osmosis—General Summary of Data

Table III presents the results of all additional reverse osmosis tests. One-point calculations of D_wC_w or D_sK were generally made, as described above. Figure 5 depicts the data for the E, ET, and TE series of membranes at 800 psig, 1% salt, 1500 psig, 4% salt, and at 1500 psig, 1% salt solutions, respectively. The general region of cellulose acetate (dense skin) performance is also shown.[6]

It should be noted that some very high salt rejections were achieved with these membranes. It can be seen in Figure 5 that increased EA content in the E series membranes leads to an increase and eventual leveling-out of salt rejection, accompanied in all cases by a decrease in $J_w(\Delta X)$. In the ET series, with one part of TPT (3.0–4.0 mole-%) in the membrane reaction mixture, much less of a drop was noted in $J_w\Delta X$, as the EA content increased in comparison to the E series membranes where no TPT was present. This behavior is very desirable, but unexpected. The addition of TPT in the TE series resulted in significant losses in the $J_w\Delta X$ flux-thickness product along with smaller increases in the salt rejection characteristics of the membranes.

Figure 6 is a logarithmic plot of D_wC_w versus D_sK for all of the reverse osmosis runs made (data from Tables II and III). The data for the ET

TABLE III
General Summary of Reverse Osmosis Results[a]

Membrane no.	ΔX, mils	$C'_{s,0}$, wt-%	$\Delta\pi$, psig	ΔP, psig	$J_w\Delta X$, (gal-mil)/-(ft²-day)	S.R., %	D_wC_w, gram/cm-sec	D_sK, cm²/sec
E-1	5.6	1.0	70.4	800	2.08	64.0	6.2×10^{-6}	1.4×10^{-7}
E-2	5.7	1.0	78.7	800	1.88	71.5	5.7×10^{-6}	7.5×10^{-8}
E-3	6.1	1.0	82.6	800	1.45	75.0	4.8×10^{-6}	5.8×10^{-8}
E-4	5.5	1.0	83.7	800	0.95	76.0	3.2×10^{-6}	3.6×10^{-8}
ET-01	7.9	4.0	362.5	1500	0.29	80.4	6.2×10^{-7}	[b]8.5×10^{-9}
ET-11	7.4	4.0	397.0	1500	0.22	88.4	4.6×10^{-7}	[b]3.4×10^{-9}
ET-31	7.2	1.0	108.7	1500	0.20	98.6	3.4×10^{-7}	2.9×10^{-10}
TE-22	6.8	1.0	107.9	1500	0.063	98.0	1.1×10^{-7}	1.6×10^{-10}
TE-32	7.3	1.0	107.9	1500	0.049	98.0	8.3×10^{-8}	1.2×10^{-10}

[a] See *Nomenclature* for explanation of symbols.
[b] Determined from one-point ratio (see text).

series fall on one curve and the data for the TE and E series fall on a second curve. Representative data[6] for dense cellulose acetate (39.8% acetylated) are shown in Figure 6 for comparison. It is interesting to note that the ET series membranes of higher EA contents appear to have slightly more favorable performance than the best cellulose acetate membranes.

All of these data show the expected companion decreases in D_wC_w and D_sK; however, the flatter shape of the ET series curve is certainly more to be desired, since a much larger drop in D_sK is achieved for any particular decrease in D_wC_w.

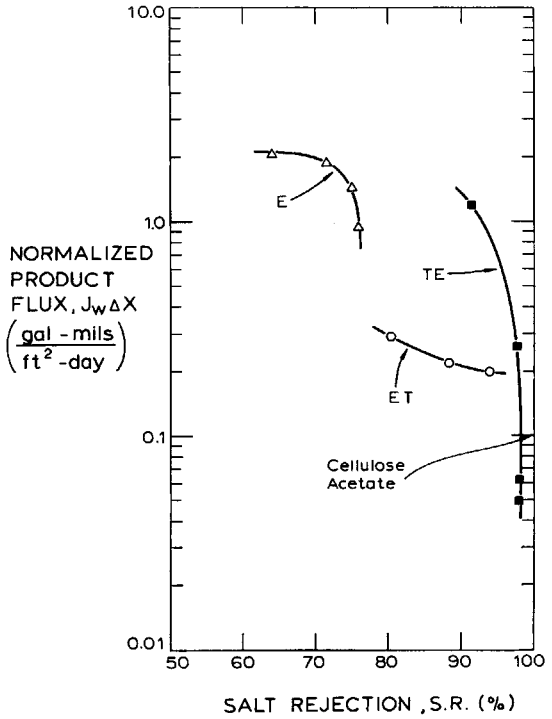

Fig. 5. Normalized product water flux as a function of salt rejection for three series of membranes.

Values of D_s and D_w may be calculated from the permeability data, and the results for the same data shown in Figure 4 are presented in Table IV and in Figure 7. The ratio D_s/D_w, the "kinetic" factor controlling salt rejection, is shown in the fourth column of the table.

In comparing data in Tables III and IV and data for K^* and C_w^* in Hoffman et al.,[1] it appears that in the E series the increase in salt rejection with increasing EA content is mainly due to a decrease in the molal salt distribution ratio K^* and thus to rapidly increasing exclusion of salt, since the ratio D_s/D_w is approximately constant. The decrease in water flux with increasing EA content is mainly due to a decrease in water content C_w^*,

TABLE IV
Diffusivities and Diffusivity Ratio[a]

Membrane no.	D_s, cm²/sec	D_w, cm²/sec	(D_s/D_w) × 10²	(D_{w_2}/D_{w_1}) × 10²
E-2	4.4×10^{-7}	1.2×10^{-5}	3.7	3.3
E-4	3.6×10^{-7}	1.0×10^{-5}	3.6	3.2
ET-01	1.1×10^{-7}	2.1×10^{-6}	5.2	5.6
ET-11	5.5×10^{-8}	1.7×10^{-6}	3.2	3.3
ET-21 (a4)	2.5×10^{-8}	1.7×10^{-6}	1.5	1.6
ET-21 (b1)	2.3×10^{-8}	1.6×10^{-6}	1.4	1.5
ET-21X (d)	2.7×10^{-8}	1.5×10^{-6}	1.8	1.9
TE-02 (b2)	1.5×10^{-7}	5.6×10^{-6}	2.7	2.8
ET-21 (a3) or TE-12 (a3)	1.1×10^{-8}	1.7×10^{-6}	0.65	0.68
TE-22	3.0×10^{-9}	4.8×10^{-7}	0.63	0.65
TE-32	2.7×10^{-9}	4.0×10^{-7}	0.68	0.72
TE-12X (c)	1.2×10^{-8}	1.6×10^{-6}	0.75	0.76

[a] The reverse osmosis conditions in this table were restricted to the following values: E series, 1% salt, 1500 psi; ET series, 4% salt, 1500 psi; TE series, 1% salt, 1500 psi.

since D_w is approximately constant and in fact close to the value for the self-diffusion coefficient of pure water, 2×10^{-5}.[7]

On the other hand, in the ET series the increase in salt rejection with increasing EA content is caused both by exclusion of salt (K^* decreases slowly as EA content increases) and by a decrease in D_s/D_w. This de-

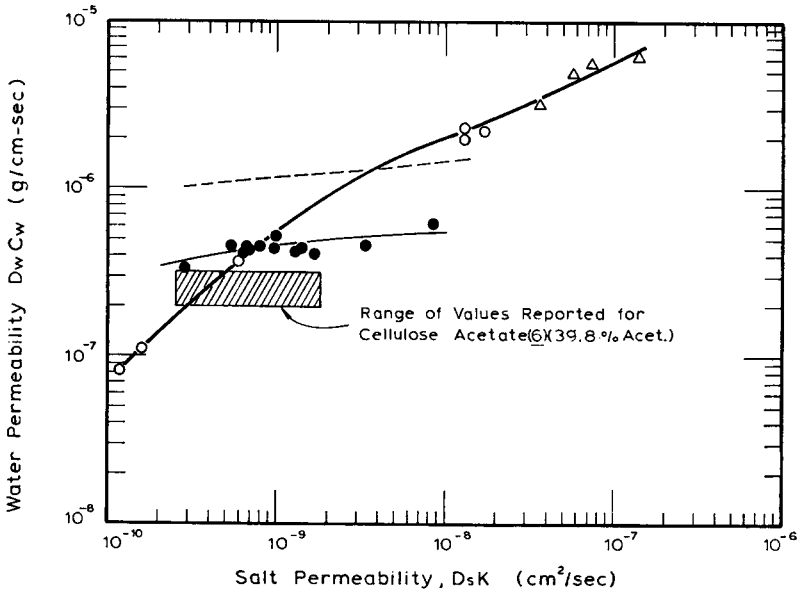

Fig. 6. Correlation of log water permeability (D_wC_w) and log salt permeability (D_sK) for all membranes studied: (○) TE series; (●) ET series; (△) E series.

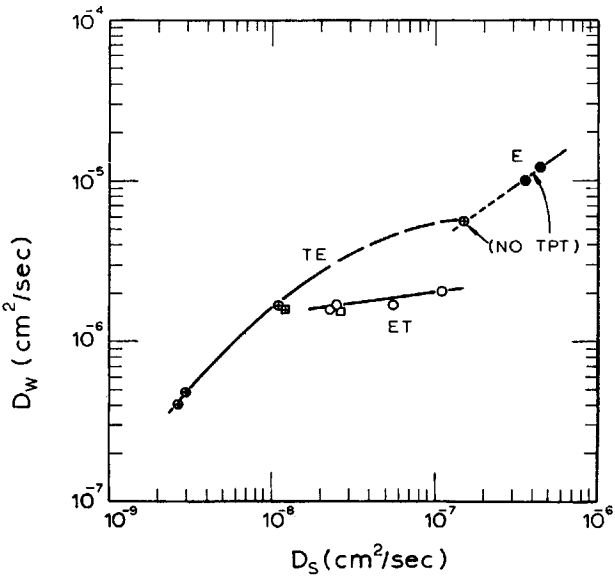

Fig. 7. Total water diffusivity vs. salt diffusivity: (⊞) TE-12X membrane; (□) ET-21X membrane.

crease in D_s/D_w is due mainly to a decrease in D_s as can be seen in Figure 7. The small decrease in water flux as EA content increases is due primarily to a decrease in water content C_w* and secondarily to a decrease in D_w.

In the TE series, the sharp increase in rejection between TE-02 and TE-12 is caused mainly by the sharp drop in D_s/D_w, and this is due to more than an order of magnitude drop in D_s (see Fig. 7). The sharp decrease in water flux between TE-02 and TE-12 is a result both of a decrease in D_w (by a factor of 3.3) and a decrease in water content C_w* (by a factor of 1.5). It is interesting to note in Figure 7 that two separate curves may be drawn, one for E-2, E-4, and TE-02, none of which contain TPT, and another for TE-12, TE-22, and TE-32, all of which contain TPT. Between TE-12 and TE-32 the salt rejection is approximately constant, but the flux continues to drop slowly; this is caused by gradual decreases in both water content C_w* and in D_w.

The effect of oven treatment on D_s or D_w is seen to be small, as the data (shown in Table IV and as squares in Fig. 7) for two of the nonheat-treated membranes are very close to those for the oven-treated membranes.

At this point it should be recalled (see Hoffman et al.[1]) that the addition of TPT in the TE series converts a rubbery membrane (all E series membranes are rubbery) first into a stiff, leathery material and then eventually into a brittle material. On the other hand, addition of EA to the membrane compositions containing TPT in the ET series converts a brittle material into an increasingly softer, more rubbery material.

Thus one may postulate that the trends of the reverse osmosis and permeability data for the ET series (e.g., Figs. 5 and 6) differ so much from the

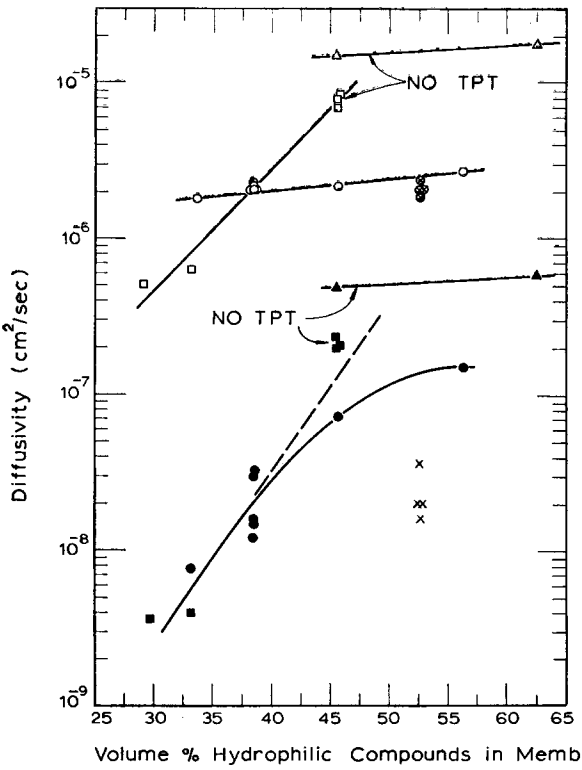

Fig. 8. Log of primary and secondary water diffusivities, D_{w_1} and D_{w_2}, as a function of membrane hydrophilic content: (○), (□), (△) D_{w_1}; (●), (■), (▲) D_{w_2}; (×) ET-21X membranes.

expected behavior as exhibited by the E and TE series because two important effects are combined: (1) increasing flexibility of the polymer chain segments paralleling a decrease in the membrane hydrophilic character, along with (2) the presence of a small amount of TPT crosslinker. The effect of the physical state of the membrane, i.e., whether it is glassy or rubbery, on desalination performance has recently been discussed.[8]

Extrapolating these observations further, it may be possible to obtain higher water permeabilities without significant loss in rejection efficiency by making membranes with TPT contents between 0 and 3–4 mole-% with increasing EA contents (for the same AAc and NMA contents in the monomer mixture). The predicted range of values of permeabilities for such a membrane series is presented by the dotted line in Figure 6.

INTERPRETATION

The trends in the data discussed above may be interpreted in molecular terms and related to the composition of the membrane by use of the primary-secondary bound water model.[1,4] In this model, we will assume that

the water is absorbed into and transported through the membrane by two independent mechanisms. Primary water is absorbed via hydrogen bonding at polymer hydrophilic sites and diffuses by an activated process from one site to another. Secondary water and the salt ions associated with it are imbibed into "clusters" or more open hydrophilic regions within the polymer matrix and diffuse together from one cluster to another across the membrane. If the salt-to-water ratio in the clusters is assumed to vary linearly across the membrane, decreasing from that in the upstream solution to that in the downstream solution at the respective interfaces, then one may calculate the average primary and secondary water contents in the membrane, $C_{w_1}^*$ and $C_{w_2}^*$, respectively.[1] It is then assumed that the diffusivities of the salt and its secondary water within the polymer matrix are in the same ratio as in the upstream or downstream dilute salt solutions, i.e., $(D_s/D_{w_2})_m = (D_s/D_w)_e \cong (1.5 \times 10^{-5})/(2.0 \times 10^{-5}) = 0.75$.[7] This equation defines D_{w_2}.

Finally, if the diffusion of primary water is assumed to be independent of that of the secondary water (and salt ions) then one may add the two permeabilities to obtain the overall water permeability, e.g., $D_w C_w = D_{w_1} C_{w_1} + D_{w_2} C_{w_2}$. This equation defines D_{w_1}. Note that the salt and secondary water are assumed to be coupled although no coupling is implied between the primary water and secondary water plus salt. The solution–diffusion model without the distinction between primary and secondary water implies a lack of coupling between salt ions and water. However, in most of the membranes studied here, the salt flux is much smaller than the total water flux; therefore it is concluded that the approximations

TABLE V
Calculated Primary and Secondary Water Diffusivities

Membrane no.	D_{w_1}, cm²/sec	D_{w_2}, cm²/sec
E-2	1.8×10^{-5}	5.9×10^{-7}
E-4	1.5×10^{-5}	4.8×10^{-7}
ET-01	2.7×10^{-6}	1.5×10^{-7}
ET-11	2.2×10^{-6}	7.3×10^{-8}
ET-21 (a1)	2.3×10^{-6}	1.2×10^{-8}
ET-21 (a2)	2.1×10^{-6}	1.6×10^{-8}
ET-21 (a3)	2.2×10^{-6}	1.5×10^{-8}
ET-21 (a4)	2.1×10^{-6}	3.3×10^{-8}
ET-21 (b)	2.1×10^{-6}	3.1×10^{-8}
ET-31	1.8×10^{-6}	7.7×10^{-9}
TE-02 (a)	7.9×10^{-6}	2.7×10^{-7}
TE-02 (b1)	8.3×10^{-6}	2.0×10^{-7}
TE-02 (b2)	7.2×10^{-6}	2.0×10^{-7}
TE-22	6.2×10^{-7}	4.0×10^{-9}
TE-32	5.0×10^{-7}	3.6×10^{-9}
ET-21X (a)	2.4×10^{-6}	2.0×10^{-8}
ET-21X (b)	2.1×10^{-6}	2.0×10^{-8}
ET-21X (c)	2.1×10^{-6}	1.6×10^{-8}
ET-21X (d)	1.9×10^{-6}	3.6×10^{-8}

involved in the primary-secondary water model will not preclude the application of the solution–diffusion mechanism.

The calculated values of D_{w_1} and D_{w_2} for all membranes are presented in Table V and are plotted as a function of the membrane hydrophilic content in Figure 8. Values of D_{w_2}/D_{w_1} are listed in the last column of Table IV, alongside of values of D_s/D_w, and can be seen to parallel the trends in this latter ratio.

It can be seen that the general trends in D_{w_1} and D_{w_2} for the three series of films are similar to those already noted for D_w and D_s, respectively. It is significant that for the ET and TE series, values of D_{w_2} appear to fall on one smooth curve for all membranes containing TPT, while separate curves are needed to distinguish the D_{w_1} values. Thus, the D_s or D_{w_2} in these membranes depends mainly on the hydrophilic content of the membrane and is only sensitive to the degree of crosslinking at the higher hydrophilic contents, while D_{w_1} (essentially D_w) is affected by both the hydrophilic content and (especially) by the degree of crosslinking. The data for the nonheat-treated films (ET-21X or TE-12X) do not fit the correlations very well, and this suggests that the hydrophilic content in these membranes has been overestimated. (Perhaps not all of the NMA groups are available for hydrogen bonding with water.)

On the basis of these observations, one may postulate the following molecular interpretation of the flux mechanisms in these membranes: If the secondary water (+ salt) resides in pockets or clusters within the polymer matrix, then for diffusion of secondary water (+ salt) to occur these species must pass from one cluster to the next, possibly through narrow, tortuous channels or capillaries of secondary water (+ salt) which connect the pockets. These capillaries are surrounded by salted-out hydrophilic groups or hydrophobic groups along the polymer chains. The rate of secondary water (+ salt) diffusion would be limited by the rate of passage through the connecting capillaries, and this is presumably the reason that D_s (or D_{w_2}) is always one to two orders of magnitude lower than D_w (or D_{w_1}). As the hydrophilic content of a membrane decreases, one would expect the number and size of clusters to decrease, and along with this the connecting capillaries should be decreased in cross section and eventually closed off. This explains the sharp decrease in D_s (or in D_{w_2}) as either TPT or EA content is increased. One would not expect the flexibility of the polymer chain segments to have a major effect on such a flux mechanism.

Primary water might be expected to diffuse by successive "jumps" along the hydrophilic groups of any one chain and by jumping from chain to chain when hydrophilic groups on neighboring chains are in close proximity. Thus, both the hydrophilic group content and the chain segmental flexibility should have major effects on the flux of primary bound water across the membrane.

Thus one concludes that the following general characteristics and approach are essential to obtain a high-flux, high salt-rejecting desalination membrane of the type studied here:

(1) The polymer composition must be designed so that it has a glass transition temperature below the use temperature, i.e., it is rubbery under desalination conditions.

(2) The membrane must contain as many random hydrophilic groups as is possible. The limit is reached when the hydrophilic content increases to a level where the hydrophilic groups will begin to cluster significantly.

(3) The membrane should be "molecularly engineered" to permit the maximum concentration of the most effective type of hydrophilic group while the hydrophobic and crosslinking monomers are varied in composition and ratio.

This research was sponsored by the Department of the Interior, Office of Saline Water, under Grant No. 14-01-0001-1256. The authors also wish to thank Dr. T. A. Jadwin and Mr. Akif Azizoglu for their assistance in the laboratory.

Nomenclature

J = flux, g/cm²-sec or gal/ft²-day
D = diffusivity in the membrane phase, cm²/sec
C_w = concentration of water in the membrane phase, g/cm³ wet membrane
C_w^* = concentration of water in the membrane phase, g/g wet membrane
$C'_{s,0}$ = concentration of salt in the upstream solution, g/cm³
$\Delta C'_s$ = salt concentration difference between upstream and downstream solution phases, g/cm³
$\bar{V}_w$ = partial molal volume of water, cm³/g-mole
R = gas constant, psi-cm³/mole °K
T = temperature, °K
ΔP = hydrostatic pressure difference across membrane, psi
$\Delta\pi$ = osmotic pressure difference for salt between upstream and downstream solutions, psi
ΔX = membrane thickness, cm
K^* = molal salt distribution coefficient, $[(\text{g salt/g water})_m]/[(\text{g salt/g water})_e]$
K = molar salt distribution coefficient, $[(\text{g salt/cc})_m]/[(\text{g salt/cc})_e]$
$(C_w)'_0$ = concentration of water in upstream solution, (g. water/g. soln.)

Subscripts

m = membrane phase
e = external solution phase
s = salt
w = water
0 = upstream solution phase
1 = primary bound water
2 = secondary bound water

Membrane Identification

EA = ethyl acrylate
TPT = trimethylol propane trimethacrylate
AAc = acrylic acid
NMA = N-methylol acrylamide
ET-21(a3), e.g. = ET series, 2 parts EA/1 part TPT, membrane "a," reverse osmosis test 3

Superscript

prime (′) = refers to external solution phases

References

1. A. S. Hoffman, M. Modell, and P. Pan, *J. Appl. Polym. Sci.*, **13**, 2223 (1969).

2. U. Merten, H. K. Lonsdale, R. L. Riley, and D. K. Vos, *Reverse Osmosis for Water Desalination*, Office of Saline Water, Research and Development Progress Report No. 208, 1966.

3. W. Banks and A. Sharples, *The Mechanism of Desalination by Reverse Osmosis, and Its Relation to Membrane Structure*, Office of Saline Water, Research and Development Progress Report No. 143, 1965.

4. B. Keilin, The Mechanism of Desalination by Reverse Osmosis, Office of Saline Water, Research and Development Progress Report No. 117, 1964.

5. U. Merten, in *Desalination by Reverse Osmosis*, U. Merten, Ed., MIT Press, Cambridge, Mass., 1966, chapter 2.

6. H. K. Lonsdale, U. Merten, and R. L. Riley, *J. Appl. Polym. Sci.*, **9**, 1341 (1965).

7. R. A. Robinson and R. H. Stokes, *Electrolyte Solutions*, 2nd ed., Academic Press, New York, 1959.

8. S. Rosenbaum, H. I. Mahon, and O. Cotton, *J. Appl. Polym. Sci.*, **11**, 2041 (1967).

Received March 19, 1969
Revised August 28, 1969